

**MINISTRY OF EDUCATION  
AND TRAINING**

**VIETNAM ACADEMY OF  
SCIENCE AND TECHNOLOGY**

**GRADUATE UNIVERSITY OF SCIENCE  
AND TECHNOLOGY**

-----



**Duong Thi Ha**

**STUDY ON ELECTROMAGNETIC WAVE ABSORPTION  
CHARACTERISTICS OF FLEXIBLE HIGH-ORDER  
METAMATERIALS IN GHz FREQUENCY RANGE**

**SUMMARY OF DISSERTATION ON ELECTRONIC  
MATERIAL**

**Code: 9440123**

*Ha Noi – 2024*

The dissertation is completed at: Graduate University of Science and Technology - Vietnam Academy of Science and Technology.

Supervisors:

1. Supervisor 1: Dr. Bui Xuan Khuyen
2. Supervisor 2: Prof. Dr. Vu Dinh Lam

Referee 1: Prof. Dr. Le Anh Tuan

Referee 2: Assoc. Prof. Dr. Nguyen Van Quy

Referee 3: Assoc. Prof. Dr. Ngo Quang Minh

The dissertation was examined by Examination Board of Graduate University of Science and Technology, Vietnam Academy of Science and Technology at 9:00 a.m. on July 03, 2024.

The dissertation can be found at:

1. Graduate University of Science and Technology Library
2. National Library of Vietnam

## INTRODUCTION

### 1. The urgency of the thesis

Metamaterial perfect absorber – MPA was first proposed in 2008. It has the advantage that the unit cell size is smaller than the absorption wavelength, high absorption efficiency, and adjustable absorption frequency range [1]. Therefore, MPAs have gained much attention for a variety of applications related to electromagnetic wave absorption, from civil to military fields in different frequency ranges [10-12]. Nowadays, the development of modern technologies of the AI (artificial intelligence), the machine learning, the 5G/6G and the IoT (internet of things) requires the development of MPA for multiple-user multiple-input and multiple-output (MIMO) approaches at lower frequency (30 MHz–10 GHz) [13]. These MPAs proceed for promising applications in energy harvesting [14], UHF-RFID systems [24], Wi-Fi devices for 4G communication [17], wearable devices [18], satellite communication, long-distance radio telecommunication and high-speed wireless channels [19] ... Besides the GHz frequency region, MPA operating in the THz frequency region is also gained much attention for many practical applications such as gas sensors [20,21], improving optical performance of infrared heaters, imaging, photo-detectors, thermoelectric devices... [22-24]. Studies on MMs in general and MPA in particular have been implemented at the Institute of Materials Science (VAST) since 2009 and has been obtained many important results. The main research directions include optimizing the resonance structure in a simple, easy-to-manufacture direction; improve/extend the operating frequency range to obtain multi-band or wide-band MPA; Actively control the absorption properties of materials by external effects...

For the problem of improving/extending the bandwidth of MPA, there are some main methods have been proposed: designing MPAs with a stacked multi-layer structure (vertical arrangement), or using a monolayer structure with a super unit cell composed of resonant structures have different sizes/shapes (horizontally arranged) [31,32], integrating components such as

resistors, diodes, capacitors [33,34] ... Such designed MPAs have complex interactions between structures and difficult experimental processes. At the same time, they have a large unit cell size and mass, so they are limited for applications that require small and lightweight MPA. To overcome these limitations, dual-band or multi-band MPAs based on high-order resonances have been proposed and actively studied in both theoretical and experimental. In addition, high-order resonance enables MPAs to be fabricated on a larger scale which is desirable for possible fabrication in the optical range. This is an effective solution that can replace complicated and expensive manufacturing techniques. Higher order resonances in MPA have been observed and investigated. However, the issue of the mechanism of high-order resonance and the ability to operate stably/actively control high-order resonance still need to be researched and clarified.

In addition, studies on the fabrication and electromagnetic characteristics of flexible MPA has been receiving attention and intense research recently [38-41]. In general, MPAs are made from flat and rigid materials, so it is difficult to change shape after fabricating. This makes it difficult to cover or integrate onto actual objects (which often have complex curved surfaces). In particular, due to inelasticity, most traditional MPAs also have limited in controlling/ensuring high performance in perfect absorber under the polarization of electromagnetic waves. Therefore, equipping MPAs with flexible features to enhance their potential application, especially in the military field, is one of the urgent requirements. However, the electromagnetic characteristics of flexible MPAs still have many issues that have not been clearly studied, especially the interactions between the unit cells and the high-order resonances in the bent state. Therefore, the thesis will solve the problem of designing multi-band, flexible MPAs, with high absorption performance that is well maintained in both flat and bent states using high-order resonance effect. Although high-order MPA and flexible MPA have been studied, there are still a number of issues that need to be further investigated and clarified, such as:

- i) Mechanisms of high-order resonances.
- ii) Tunable high-order resonances.
- iii) Characteristics of high-order resonance in flexible MPA, in different curved states.

With the advantages of high-order resonance discussed above, this thesis focuses on clarifying the mechanism of high-order resonance in MPA, aiming to design and fabricate high-order MPA that operates stably or can be actively controlled, and investigating the high-order resonance effects in flexible MPA. This is one of the important research directions in the process of realizing the application potential of MPA.

## **2. The objectives of the thesis**

- Clarifying the physical mechanism of high-order MPA and flexible MPA.
- Designing, fabricating multi-band MPAs using the high-order magnetic resonance effect and flexible MPAs, operating in the low frequency region (from 0.1 to 12,0 GHz).
- Apply optimized models to design flexible MPAs operating in the THz frequency range.

## **3. New contributions of the thesis**

- i) Clarifying the physical mechanism of high-order MPA and flexible MPA.
- ii) Designing and manufacturing a number of multi-band H-MPAs using odd-order magnetic resonance effects (third- and fifth-order) operating in different frequency bands, from VHF band (0,03-0,30 GHz) to S band (2.0 - 4.0 GHz) with absorption over 90%. Successfully designing and manufacturing a number of flexible, high-order metamaterial perfect absorbers operating in the C (4.0 – 8.0 GHz) and X (8.0 – 12.0 GHz) bands. The proposed structure activates the second-order magnetic resonance effect for bending state.
- iii) The thesis carried the further study on H-MPAs operating in the higher frequency region (THz) to clarify the dependence of the absorption

spectrum on the different curved states. In flat state, there are two absorption peaks: the fundamental resonance peak at 34.9 THz with the absorption of 96% and the third-order resonance peak at 97.2 THz with absorption of 99.2%. Since the bending radius reduces to be 5  $\mu\text{m}$ , a second-order resonance peak is activated at 54.5 THz with absorption of 80%.

## **Chapter 1. OVERVIEW OF HIGH-ORDER RESONANCE AND FLEXIBLE METAMATERIAL PERFECT ABSORBER**

### **1.1. Overview of Metamaterial perfect absorber (MPA)**

#### **1.1.1. History and development of MPA**

MPA was first proposed by Landy *et al.* in 2008 [9]. Since then, research on electromagnetic wave absorbers based on MMs has been of great interest and development with many different research directions such as optimizing the structure towards simplicity, easily in fabrication; improving/extending the bandwidth of MPA, and so on.

#### **1.1.2. Classification of MPA**

Based on the operating frequency band, MPAs can be classified into three types: single-band, multi-band, and broadband MPAs. Depending on the application purpose, these MPAs are designed to obtain the appropriate absorption band. Typically, MPAs exhibit narrow-band or single-band absorption characteristics. Multi-band MPAs can be achieved by arranging the resonance structures horizontally or vertically [37,80]. There are four main methods to achieve broadband characteristics: horizontal arrangement of resonant structures; multilayer structure design; using lumped elements such as resistors, capacitors and exploiting plasmonic materials [81-88].

#### **1.1.3. Electromagnetic wave absorption mechanism of MPA in GHz range**

##### **\* Impedance matching theory**

Since the electromagnetic waves (EMWs) encounter materials, the wave will be partially reflected, partially transmitted and partially absorbed. If the effective impedance of material matches the values of the environment medium, the impedance matching condition is satisfied leading to the

reflection is minimized to be zero. In this condition, all EMWs penetrate through into the material. By blocking the transmission based on continuous metallic plates, the total energy of incoming EMWs can be consumed inside the MPAs at around the impedance-matching frequencies.

### \* **Interference theory**

At the free space-MPA interface, the incident light is partially reflected back to air and partially transmitted into the MPA. The latter continues to propagate until it reaches the ground plane and form a secondary reflection. When the dielectric layer reaches a critical thickness, the secondary reflection and the first reflection are in opposite phase and have the same amplitude, destructive interference occurs, leading to perfect absorption [92].

## **1.2. Higher-order resonance theory in MPA**

### **1.2.1 Electromagnetic characteristics of high-order metamaterial perfect absorber (H – MPA)**

Consider the simple case, a CWP structure with the edges parallel to the E and H axes of the incident electromagnetic wave. The CWP structure reveals multiple peaks at 3.87 GHz (40.31%), 11.52 GHz (50.81%), 18.54 GHz (48.23%), and 27.15 GHz (47, 34%). These peaks correspond to fundamental, the third-, fifth-, and seven-order magnetic resonances [42].

### **1.2.2. The differential equivalent-circuit method applies to high-order resonances in MPA**

The absorption mechanism and characteristics of odd-order magnetic resonance can be elucidated through the differential equivalent circuit (DEC) method, in which the MPA is subdivided into N domains. Each domain is substituted with infinitesimal circuit components [42]. By solving the circuit based on Kirchhoff's laws, three types of resonance become a solution at  $N \rightarrow \infty$  ( $\phi \rightarrow 0$ , simultaneously): (1) odd-order magnetic resonances, (2) even-order magnetic resonances and (3) electric resonances. For the case of magnetic resonance, the surface currents on both sides of the metal are opposite. However, the surface currents in the two metal layers are in the same direction for electric resonance.

### **1.3. Electromagnetic characteristics of H-MPA structures**

#### **1.3.1. H-MPA based on disk and ring-shaped resonators**

By optimizing the geometric parameters, disk and ring-shaped resonant structures can produce high-order magnetic resonances including third- and fifth-order magnetic resonances [41,96].

#### **1.3.2. H-MPA based on flower-shaped**

The flower-shaped resonators also provide high-order resonances and produce multi-band absorption [40]. The number of absorption peaks of this H-MPA can be increased by choosing appropriate geometrical parameters of the unit cell structure.

### **1.4. Improving performance of MPA based on flexible material**

#### **1.4.1. Flexible MPA based on Polyimide**

Polyimide is a type of polymer with good heat resistance, high mechanical strength, and good flexibility, therefore, it is widely used in constructing MPAs with elastic properties, expanding the application potential of MPAs in practice [46,101].

#### **1.4.2. Flexible MPA based on Polydimethylsiloxane (PDMS)**

Polydimethylsiloxane (PDMS) is an advanced material with a high surface energy, good biocompatibility and flexibility. It is a suitable substrate for flexible MPA, which can be controlled by both bending and stretching impacts [104,105].

#### **1.4.3. Flexible MPA based on paper**

Paper can be easily folded or bent into different shapes, meeting many designs for different applications. Therefore, it is considered as an ideal substrate for a thin, flexible and lightweight MPAs, with controllable electromagnetic properties [106-109].

### **1.5. Conclusions**

To achieve multiband MPA while preserving the compact size and mass, MPA based on high-order resonance have been proposed. However, to expand the application potential of H-MPA, some further researches need to be carried out such as integrating H-MPA onto flexible dielectric



substrates and optimizing the structure to maintain good absorption properties under large incident angles. Therefore, the thesis focuses on designing and studying the electromagnetic properties of H-MPA integrated onto a flexible polyimide substrate. The resonance structures are square-shaped, ring-shaped for simple fabrication. In addition, these structures are improved into integrated capacitor, two squares rotated at an angle of 45 degrees and folded ring resonance to obtain multi-band H-MPA, operating in different frequency regions, from VHF band to THz. The electromagnetic properties of H-MPA were investigated for both flat and bent configurations.

## **Chapter 2. RESEARCH METHODS**

In this thesis, we study electromagnetic characteristics of H-MPA using a combination of methods: simulation, theoretical calculation, and experiment. These methods are highly reliable and have been widely used in the field of research on MMs.

### **2.1. Simulating the electromagnetic properties of flexible H-MPA**

The electromagnetic characteristics of H-MPAs are simulated using the physics simulation software CST (Computer Simulation Technology). Based on the finite integration technique, the scattering parameters  $S_{11}$  and  $S_{21}$  are determined. In addition, the surface current distribution, electric and magnetic field distributions, etc. are extracted. Consequently, the electromagnetic properties of H-MPA can be analyzed.

### **2.2. The model for calculating the effective parameters of H-MPA**

#### **2.2.1. The LC equivalent - circuit model**

Under the polarization of incident EMWs, H-MPA acts as an equivalent LC-oscillator circuit. In which, conductive components are modeled as inductors and the interactions between metallic or conductive components are modeled as capacitors. The fundamental and high-order resonant frequencies of MPA can be determined by the natural oscillation frequencies of the LC circuits [95].

#### **2.2.2. Calculating the effective impedance**

To examine the impedance matching condition, the effective impedance of the MPA is calculated from the scattering parameters according to the

method proposed by Chen *et al.* [114]. The impedance matching condition is satisfied when the effective impedance has a real part of 1.0 and an imaginary of 0.

### **2.3. Experimental method of H-MPA operating in GHz range**

For H-MPAs with a metal - dielectric - metal structure, in the GHz frequency range, the fabrication method is chosen as the photolithography. This method includes four main steps: Exposure, Development, Etching or Implantation, and Photoresist removal. For the case of resonant structures made from conductive ink, the method is chosen as stencil printing.

### **2.4. Experimental method to evaluate the electromagnetic characteristics of H-MPA**

The experimental results of the thesis were measured at the Institute of Materials Science, Vietnam Academy of Science and Technology, using the Rohde & Schwarz ZNB20 Vector Network Analyzer equipment. Experimental results are expressed in terms of reflection and absorption of MPA can be determined by:  $A = 1 - R$ , where  $R$  is the reflection.

### **2.5. Conclusions**

The thesis uses a combination of research methods of physical simulation, modeling using LC circuits, and experiment. These are effective methods to study the electromagnetic characteristics of common MPAs and H-MPAs. The above research methods were carried out independently and compared to verify and ensure the accuracy of the results.

## **Chapter 3. THE ABSORPTION CHARACTERISTICS OF THE ODD-ORDER RESONANCE METAMATERIALS**

This chapter presents a number of H-MPA structures with improved surface structures including capacitor integration, folded resonant ring and star – shaped (two squares rotated 45° apart) to obtain multi-band absorbers based on the odd-order resonances. These H-MPA work in the VHF - S bands (0.03 – 4 GHz) and THz band. In addition, this structure is integrated onto flexible polymer substrate to expand their application possibilities in reality.

### 3.1. The absorption characteristics of H-MPA integrated capacitors operating in both VHF- band (30 - 300 MHz) and S- band (2,0 - 4,0 GHz)

#### 3.1.1. The absorption characteristics of H-MPA based on square-shaped resonator, without capacitor

Firstly, the electromagnetic characteristics of H-MPA based on the periodically square-shaped resonators with the FR-4 dielectric layer are considered. The simulation results show that, there are two peaks at 2.05 and 6.06 GHz (Fig. 3.1). The surface current distribution shows that the peak at 2.05 GHz originates from the fundamental magnetic resonance, the peak at 6.06 GHz is derived from third-order magnetic resonance.

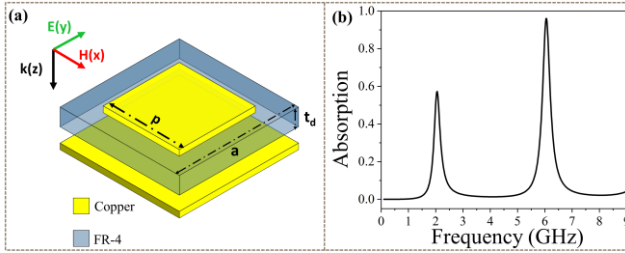


**Figure 3.1.** (a) Unit cell structure of H-MPA, (b) Simulated absorption spectrum of H-MPA with dielectric thickness of  $t_d = 3$  mm.

#### 3.1.2. The absorption characteristics of the integrated capacitors H-MPA

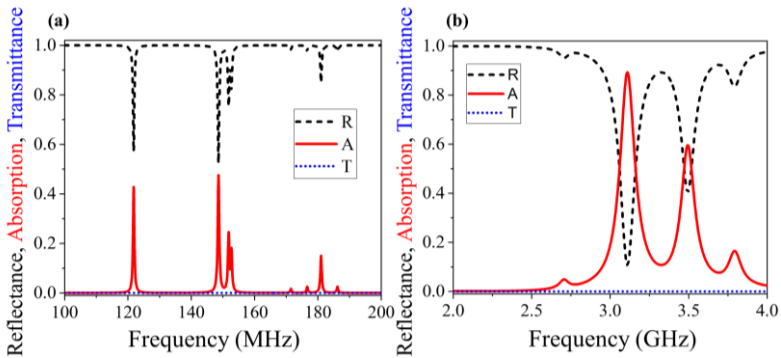


**Figure 3.9.** Reflection ( $R$ ), absorption ( $A$ ) and transmittance ( $T$ ) spectra of a capacitor-integrated H-MPA in (a) VHF and (b) S-band.

When capacitors  $C_1$  (capacitance 180 pF) and  $C_1$  (capacitance 360 pF) are integrated into the gaps between square-shaped resonators, there are two

fundamental absorption peaks in the VHF frequency region. At the same time, it also exhibits two high-order absorption peaks in the S band.

### 3.1.3. Investigating the effect of capacitors on the absorption properties

As capacitance of  $C_1$  and  $C_2$  increase, the absorption peaks in the VHF band shift toward lower frequencies. In particular, the high-order absorption peaks in the S band do not depend on the capacitance of  $C_1$ , and  $C_2$ .

### 3.1.4. The influence of the electromagnetic wave incident angle on the high-order absorption characteristics of H-MPA in the S band

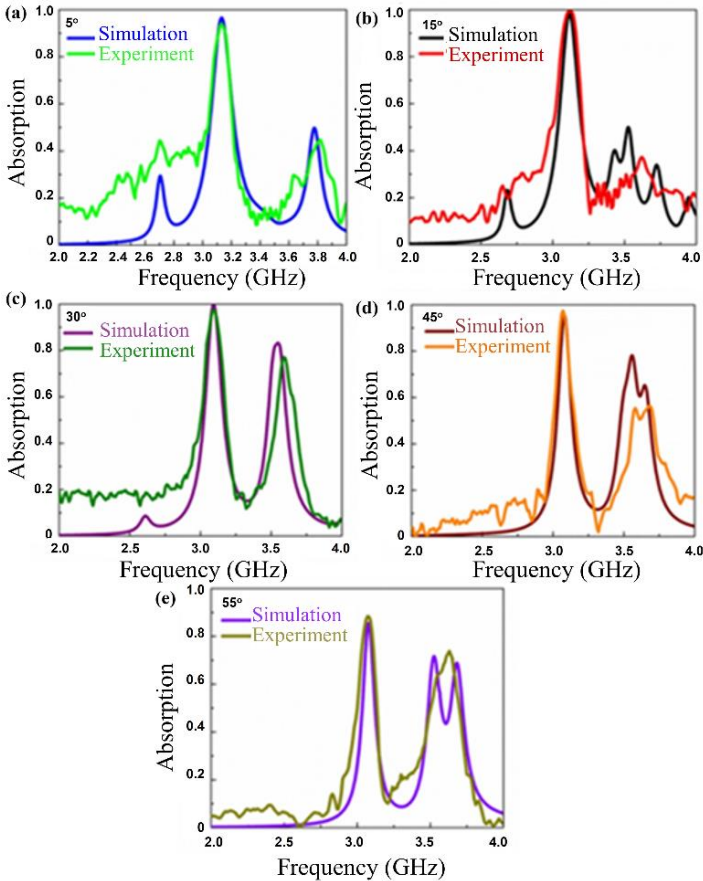


**Figure 3.17.** Evolution of the absorption at different incident angles of the EM wave (2.0–4.0 GHz): (a) 5°, (b) 15°, (c) 30°, (d) 45° and (e) 55°.

Experimental results show that the proposed structure has two high-order absorption peaks at 3.13 (93.9%) and 3.82 GHz (44.7%). When the incident angle increases from 0 to 30°, the absorptivity of these peaks increases. If the incident angle is up to 45°, a new peak appears at 3.67 GHz with an intensity of 56.5%. When the incident angle increases to 55°, there are three absorption peaks at 3.07 GHz (88.3%), 3.54 GHz (63.9%) and 3.63 GHz (73.8%). The origin of these new absorption peaks is due to the fifth order magnetic resonance.

### 3.2. The absorption characteristics of flexible H-MPA operating in the UHF (300 MHz – 1000 MHz) and L (1,0 – 2,0 GHz) bands

#### 3.2.1. Simulation and design the flexible H-MPA

The structure of H-MPA is shown in Figure 3.19. The geometric parameters are optimized to be:  $a = 55,0$ ;  $p = 54,5$ ;  $t_d = 4,0$ ;  $w_1 = 2,8$ ;  $w_2 = 0,6$ ;  $w_3 = 0,5$ ;  $l_1 = 7,2$ ;  $l_2 = 6,5$ ;  $l_3 = 13,5$ ;  $l_4 = 20$  mm.

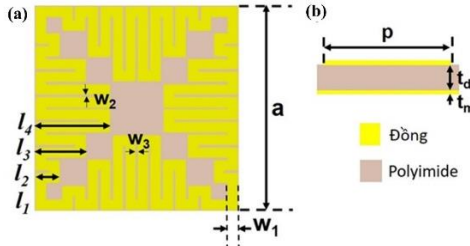


**Figure 3.19.** Illustration of the unit cell of H-MPA (a) top view and (b) side view.

#### 3.2.2. Absorption characteristics of third-order resonance H-MPA in the flat state

In the flat configuration, when electromagnetic wave is perpendicular to the surface of the structure, there are two absorption peaks at of 450 MHz and 1.47 GHz with intensities of 99.4% and 99.8%, respectively. From the effective impedance calculation results illustrated in Figs. 3.20(b) and 3.20(d), it can be seen that the impedance matching condition has been satisfied. Therefore, at 450 MHz and 1.47 GHz, the reflected component of the EMW is close to zero, almost all the incident wave is transmitted inside the H-MPA and to be totally absorbed.

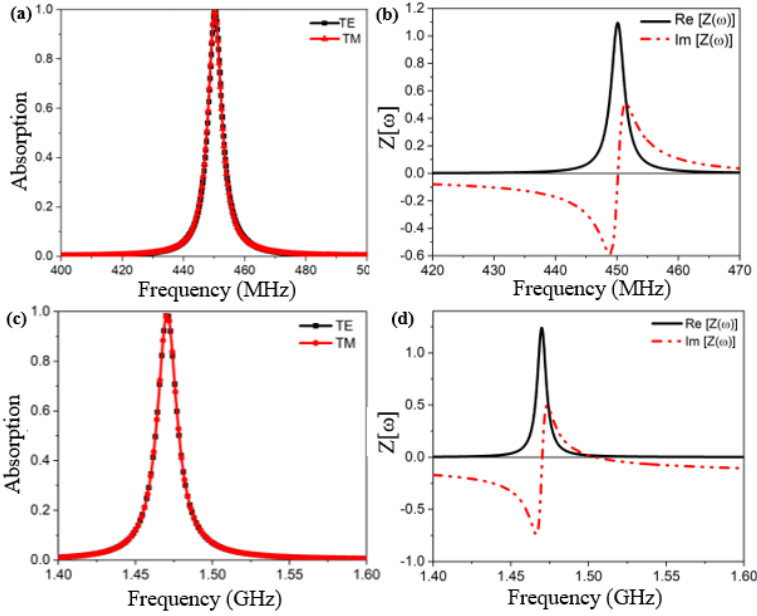


**Figure 3.20.** (a) Absorption spectrum and (b) effective impedance of H-MPA in the UHF band, (c) Absorption spectrum and (d) effective impedance of H-MPA in the L band.

### 3.2.3. The absorption characteristics of H-MPA in different deformation states

In the bending state, the absorption of the fundamental absorption peak at 450 MHz drops sharply from about 99.4% to 10%. However, a new fundamental peak appears at 556 MHz. The absorptivity of this new peak gradually increases as  $R$  decreases. When  $R = 200$  mm, the absorption of this new peak reaches nearly 90% [Fig. 3.24(a)].

When the H-MPA is bent, the high-order absorption peak at 1.47 GHz is divided into two absorption peaks, at 1.47 and 1.48 GHz. These two peaks originate from third-order resonance. As  $R$  decreases to 200 mm, the absorption at 1.48 GHz increases to be nearly 79%, while the absorption of initial high-order peak is nearly unchanged [Fig. 3.24(b)]. The formation of new higher-order absorption peaks is explained by the asymmetric structure at different bending states [118].

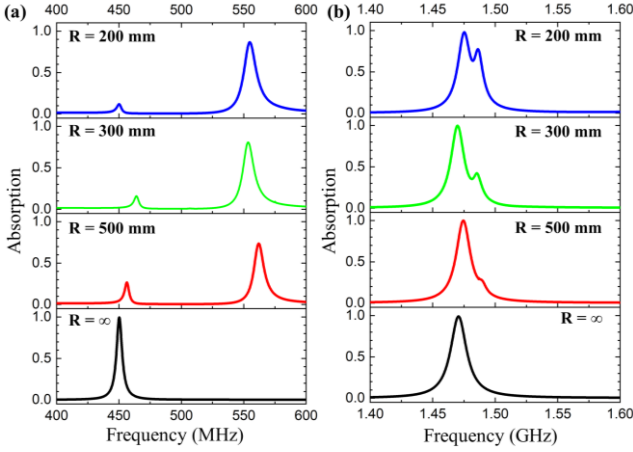


**Figure 3.24.** Dependence of the simulated absorption spectrum on the bending radius for (a) fundamental and (b) high - order absorption peaks.

### 3.3. The absorption characteristics of H-MPA in the THz region

#### 3.3.1. Structural of flexible H-MPA operating in the THz region

The structure of the proposed H-MPA is illustrated in Fig. 3.26. The geometric parameters are optimized to be:  $a = 2.0$ ,  $p = 1.1$ ,  $t_m = 0.07$  and  $t_d = 0.02 \mu\text{m}$ .

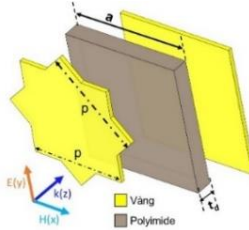


**Figure 3.26.** The unit cell structure of the proposed H-MPA operating in the THz frequency range.

#### 3.3.2. The absorption characteristics of the proposed H-MPA

The absorption spectra show a fundamental absorption peak at 34.9 THz and a third-order absorption peak at 97.2 THz with absorption of 96.4% and 99.2%, respectively [Fig. 3.27(a)]. At these two frequencies, the impedance matching condition is all satisfied [Fig. 3.27(b)], resulting in nearly perfect absorption peaks.

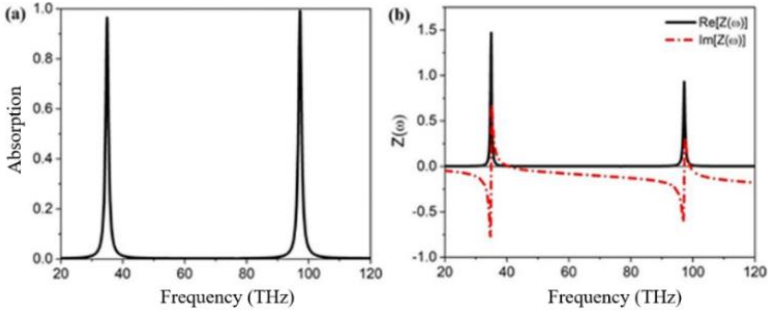


**Figure 3.27.** (a) Simulated absorption spectrum and (b) effective impedance of the proposed H-MPA.

In the curved configuration, the position and intensity of the fundamental absorption peak is unchanged. In different configurations (bending radius is reduced from 50 to 5  $\mu\text{m}$ ), the H-MPA is maintained the fundamental absorption peak with absorption above 90%. Particularly, a new second-order resonance peak is appeared at 54.5 THz with absorption of 80%.

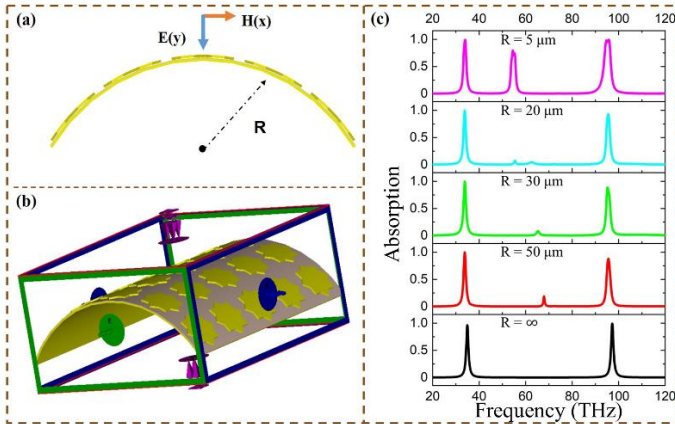


**Figure 3.31.** (a) The definition of the bending radius  $R$ , (b) the bending configuration in the simulation, and (c) the absorption spectrum in the bent state with different bending radii.

**3.4. Conclusions:** This chapter has been conducted with the target of designing and investigating the absorption properties of multi-band H-MPA, operating in various frequency bands:



i) Successfully designing and manufacturing multi-band H-MPA with integrated capacitors on the material surface. This H-MPA has two fundamental absorption peaks in the VHF and two fifth-order absorption peaks in the S bands. The high-order absorption peaks are quite sensitive to the angle of incidence.

ii) The multi-band flexible H-MPA with the folded ring resonance structure have been optimized: the proposed structure shows a fundamental peak at 450 MHz (99.4%) and a third-order peak at 1.47 GHz (99.8%). For the bending state, the absorption of fundamental peak gradually decreases and a new peak appears at 556 MHz. The absorptivity of this new peak increases as the radius  $R$  decreases. The absorption of the high-order peak is still well maintained when changing the bending radius, and there is a new absorption peak that appears at higher frequency 1,48 GHz.

iii) The absorption properties of a H-MPA in the THz region have been designed and optimized. By using the structure consisting of two squares rotated an angle of  $45^\circ$ , the absorption reaches over 96% at 34.9 THz (fundamental magnetic resonance) and 97.2 THz (third-order magnetic resonance). In different configurations (bending radius is reduced from 50 to 5  $\mu\text{m}$ ), in which the fundamental absorption peaks are maintained the absorption rates over 90%.

## **Chapter 4. ABSORPTION CHARACTERISTICS OF FLEXIBLE EVEN-ORDER METAMATERIALS**

In this chapter, the results on the absorption properties of flexible H - MPA are presented. In particular, the absorption characteristics of the even-order resonance magnetic resonance peaks depending on the bending state of the material are also investigated.

### **4.1. The absorption characteristics of flexible H-MPA based on second-order magnetic resonance**

#### **4.1.1. Designing a second-order magnetic resonance H-MPA structure**

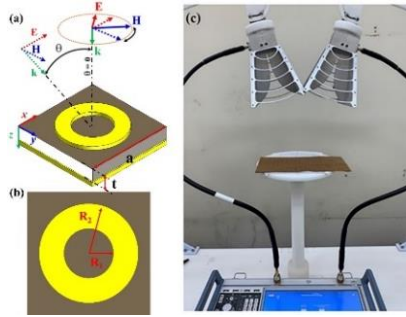


**Figure 4.1.** (a) Unit-cell of the proposed H-MPA, (b) top view, (c) measurement configuration.

The proposed H-MPA structure is illustrated as in Fig. 4.1. The geometric parameters are optimized to be:  $a = 16,0$ ;  $R_1 = 7,0$ ;  $R_2 = 6,0$ ;  $t = 0,4$  mm.

#### 4.1.2. The absorption characteristics of second-order H-MPA in the flat state

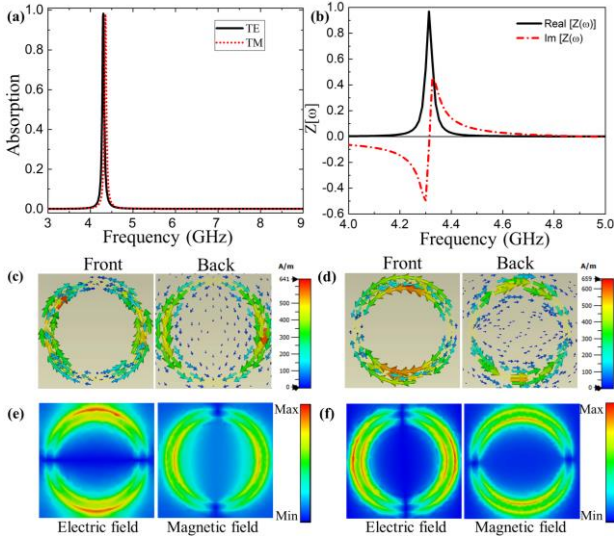


**Figure 4.4.** (a) Absorption spectrum of H-MPA, (b) effective impedance, (c) Surface current distribution and (e) electric and magnetic field distribution at 4.3 GHz with TE-polarized electromagnetic wave, (d) Surface current distribution and (f) electric and magnetic field distribution at 4.3 GHz with TM-polarized EMW.

In both cases of TE and TM polarizations, the absorption spectrum has a single peak at 4.3 GHz with the absorption of 98%. This absorption peak originates from fundamental magnetic resonance (Fig. 4.4).

For both TE and TM-polarized EMWs, when the incident angle increases from 0 to 60°, the absorption peaks at 4.3 GHz are nearly unchanged and absorptions are still maintained to be 90%. Besides, a new peak is appeared at 8.6 GHz with absorption of 63% (for the TE polarization) and at 8.7 GHz with absorption of 98% (for the TM polarization).

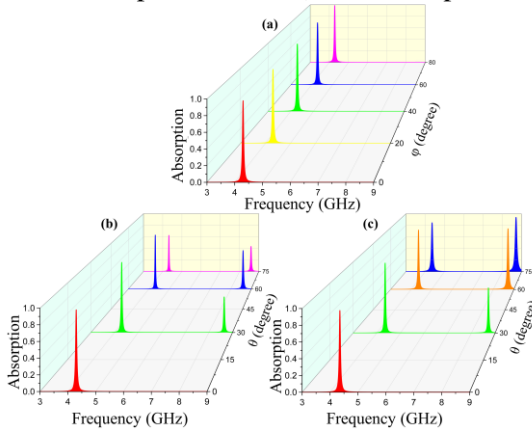


**Fig 4.6.** Simulated absorption as a function of (a) polarization angle ( $\varphi$ ) and (b) incidence angle ( $\theta$ ) for the TE polarization. (c) Simulated absorption according to incidence angle for the TM polarization.

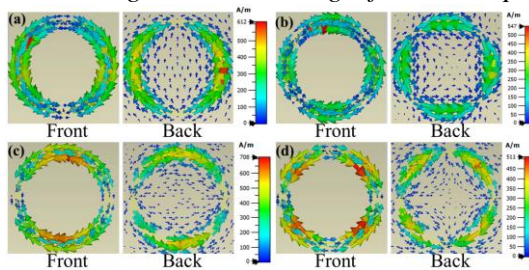


**Figure 4.7.** Surface currents at a frequency of (a) 4.3 and (b) 8.6 GHz in TE mode; (c) those at a frequency of 4.3 and (d) 8.7 GHz in TM mode.

The appearance of the new peaks can be explained by the phase retardation caused by the oblique incidence [43,115]. When the incoming

wave is not normal to the MA surface, the MA is considered to be asymmetric under the oblique incidence. The field distribution is not in phase on the whole surface. As a result, a high-order resonant mode is excited. From the surface current distribution in Fig. 4.7, the new absorption peak is owing to be the second-order magnetic resonance [118].

#### 4.1.3. The absorption characteristics of second-order H-MPA in the bent state

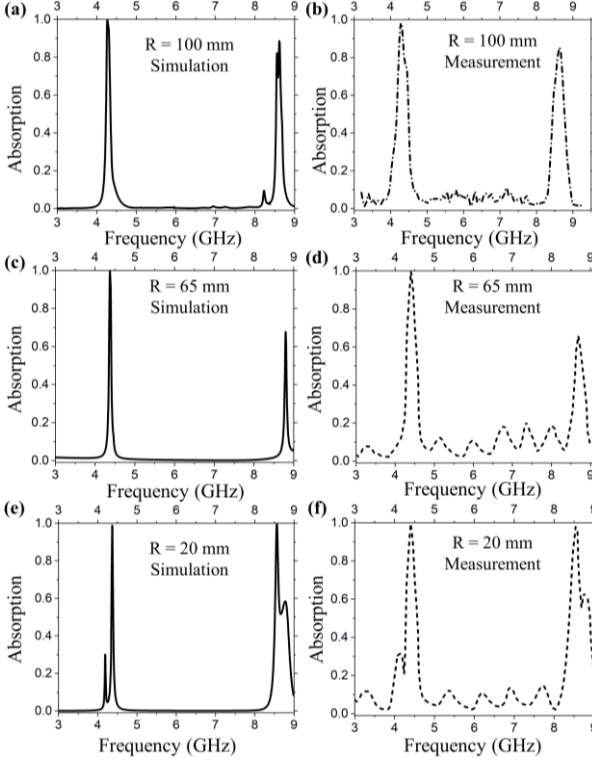


**Figure 4.10.** Simulated (a), (c), (e) and experimental (b), (d), (f) absorption spectra of H-MPA with bending radius varying from  $R = 100$  mm to  $R = 20$  mm for TE polarization.

The absorption characteristics of H-MPA in the bent state were simulated and measured with the bending radius varying from 100 to 20 mm. In the case of TE polarization, the fundamental absorption peak at 4.3 GHz is maintained to be unchanged with absorption over 99%. When  $R = 100$

mm, the simulated absorption spectrum shows two new peaks at 8.56 GHz (82.1%) and 8.62 GHz (87.3%), meanwhile, experimental spectra observed a new peak at 8.64 GHz (81.6%). When  $R = 65$  mm, a new absorption peak appears at 8.8 GHz (67.5%) in simulation, and at 8.7 GHz (66.7%) in experiment. When  $R = 20$  mm, there are three new absorption peaks at 4.2, 8.6 and 8.8 GHz, with absorption of 30%, 99% and 58%, respectively in simulation. The experimental results confirm three absorption peaks at 4.1, 8.5 and 8.7 GHz with absorption of 31.5%, 97.8% and 62.88%, respectively.

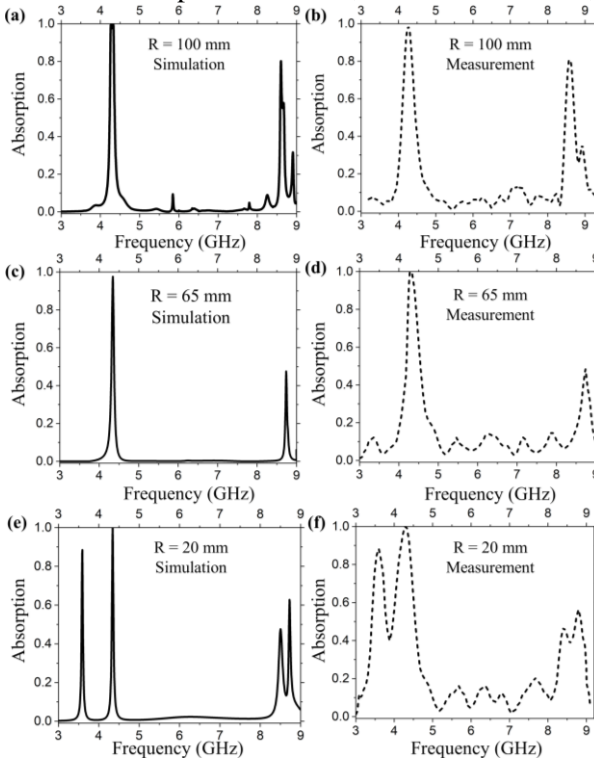


**Figure 4.11.** Simulated (a), (c), (e) and experimental (b), (d), (f) absorption spectra of H-MPA with bending radius varying from  $R = 100$  mm to  $R = 20$  mm for TM polarization.

For TM-polarization, since  $R = 100$  mm, there are two new peaks at 8.6 GHz (80.08%) and 8.9 GHz (32%) in simulation, and two new peaks at 8.6 GHz (80.1%) and 8.9 (33.7%) in experiment. When  $R = 65$  mm, a new

absorption peak appears at 8.73 GHz (46.67%) in simulation and at 8.7 GHz (45.4%) in experiment. When  $R = 20$  mm, three new absorption peaks appear around the frequencies of 3.6 GHz (88%), 8.5 GHz (47%) and 8.7 GHz (62%) in simulation and at 3.6 GHz (87%), 8.4 GHz (46%) and 8.8 GHz (55.9%) in experiment. These new absorption peaks originate from the second-order magnetic resonance, excited due to the bending making the H-MPA structure asymmetric [118,125]. The fundamental absorption peak is still well maintained with absorption of 99% in both simulation and experiment.

It can be seen that the simulation and experimental results are in good agreement with each other: the experimental results have achieved the number of absorption peaks, the peak positions have a small deviation. However, the experimental absorption is smaller than the simulation results. The reason for this difference is that the parameters of the dielectric constant and loss tangent of the manufacturer are different from the simulation parameters. In addition, the manufacturing process may encounter some errors.

## 4.2. Second-order magnetic resonance in a folded resonance structure

### 4.2.1. Design and fabrication

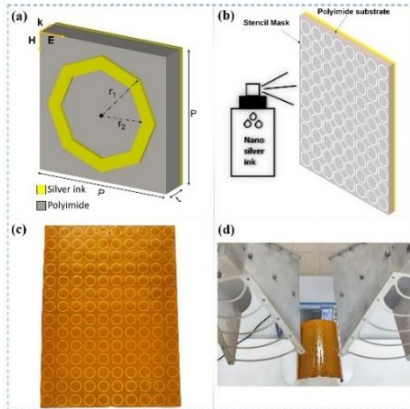


**Figure 4.14.** (a) Schematic of a unit cell of the proposed structure, (b) schematic of fabricated process, (c) fabricated H-MPA and (d) measurement configuration.

The resonance structure of the material is folded into a regular octagon, made from silver nano-ink with an electrical conductivity of  $10^7$  S/m and a thickness of 0.035 mm. The middle layer is made from the polyimide and the bottom layer is a continuous copper plane. The optimized geometric parameters include:  $r_1 = 8.5$  mm;  $r_2 = 7.5$  mm;  $t = 0.5$  mm (Fig. 4.14).

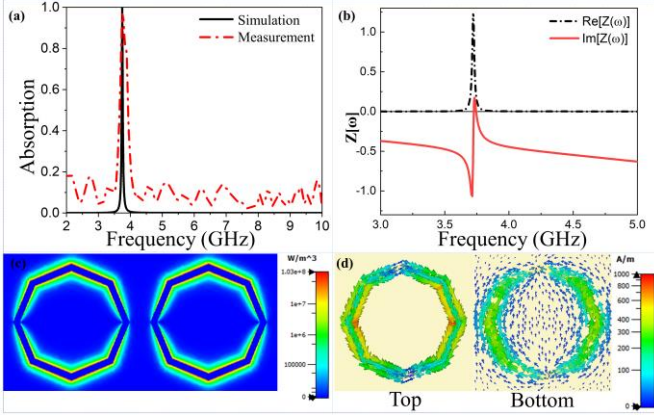


**Figure 4.15.** (a) Simulated absorption, reflection and transmission, (b) effective impedance of the proposed MPA, (c) power loss density and (d) surface currents at 3.7 GHz.

There is an absorption peak of 3.7 GHz with an absorption of 99.9% in simulation and 98% in experiment. At this frequency, both reflectance and transmittance are simultaneously zero, leading to an absorption peak near unity, confirms that the impedance matching condition is satisfied. This absorption peak originates from fundamental magnetic resonance (Fig. 4.15).

#### 4.2.2. The influence of geometric parameters and polarization angle on the absorption characteristics of material in the flat state

The influence of geometric parameters on the absorption characteristics of this H-MPA is investigated by simulation. When the thickness of dielectric layer  $t_d$  increases from 0.3 to 0.7 mm, the position of the absorption peak shifts slightly toward higher frequencies. However, the absorption changes significantly and reaches a maximum when  $t_d = 0.5$  mm (absorption of 99.5%). When the ring width ( $w = R_1 - R_2$ ,  $R_1 = 8.5$  mm) is increased from

1.0 to 4.0 mm, the absorption is decreased to be below 90%, and the absorption peak is shifted toward to the higher frequencies.

#### 4.2.3. Second-order magnetic resonance under oblique electromagnetic waves

For both TE- and TM-polarizations, when the incident angle is increased to be  $60^\circ$ , the fundamental absorption peak at 3.7 GHz is still maintained to be over 80%. Particularly, a new peak is created at 7.5 GHz. The origin of this new peak was clarified based on the surface current distribution at 7.5 GHz, where it can be revealed that it originates from second-order magnetic resonance [118,125], similar to the case of circular resonance rings.

#### 4.2.4. Second-order magnetic resonance in bending configuration

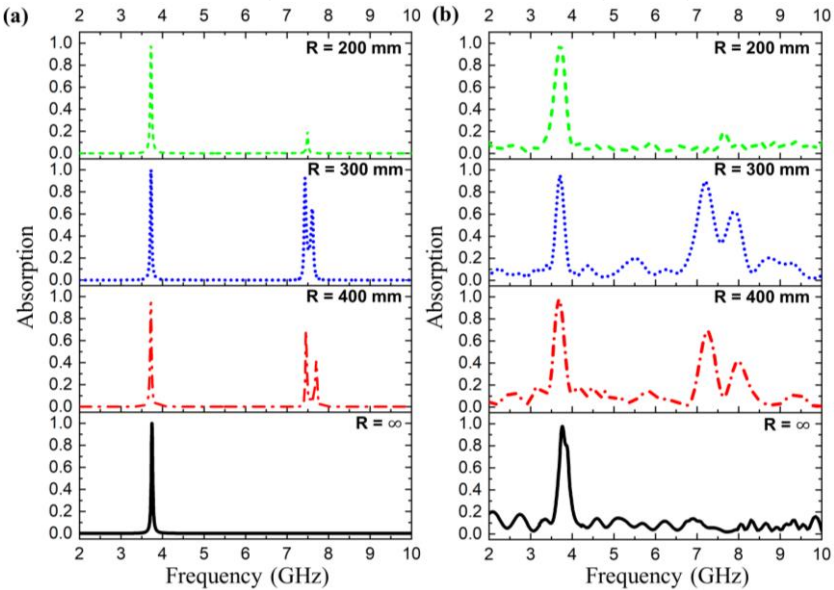


**Figure 4.24.** (a) Simulated and (b) measured absorption spectra of the H-MPAs with a decreasing bending radius from  $R = \infty$  to  $R = 200$  mm.

When H-MPA is changed to be deformation state (by different bending radius), the fundamental peak is nearly unchanged (absorption of 99% around 3.7 GHz). However, two new peaks emerge at higher frequencies.



Particularly, when  $R = 400$  mm, there are two new peaks in both simulated spectrum (absorption of 69% and 41% at 7.43 GHz and 7.6 GHz, respectively) and experimental one (absorption of 69% at 7.26 GHz and 40.8% at 8.0 GHz). When  $R = 300$  mm, two new peaks are achieved at 7.43 GHz (92.6%) and 7.6 GHz (65%) in simulation, and at 7.2 GHz (91%) and 7.9 GHz (64.1%) in experiment. However, when  $R = 200$  mm, these two new peaks merge into a single peak located at 7.5 GHz in simulation and at 7.6 GHz in experiment, leading to decreased absorption of 20%.

The distribution of induced surface currents shows that, the new peaks at higher frequencies can be originated from second-order magnetic resonances, which are caused by the bent state of the H-MPA structure. It can be regarded as an inhomogeneous distribution of electric and magnetic fields on the H-MPA surface is activated [118].

### 4.3. Conclusions

In this chapter, we have designed and investigated the electromagnetic characteristics of flexible H-MPA in the GHz region with resonant structures of ring-shaped and octagonal-shaped. By optimizing the geometric parameters, second-order magnetic resonances can be excited under oblique incidences or when the material is bent.

## CONCLUSIONS

The thesis "*Study on the electromagnetic wave absorption characteristics of flexible high-order metamaterials in the GHz frequency range*" was carried out at the Institute of Materials Science and the Academy of Science and Technology, Vietnam Academy of Science and Technology. The results of the thesis have been published in journals including: 02 articles in ISI magazine, 02 articles in domestic journals, 01 article in the proceedings of national specialized conferences.

The thesis has completed the objectives and obtained some main results:

1. Clarifying the operating mechanism of multi-band H-MPAs based on high-order magnetic resonance and flexible H-MPAs.

2. Designing and successfully manufacturing a number of multi-band H-MPAs based on high-order magnetic resonance:

+ H-MPA with embedded capacitors: there are two fundamental peaks in the VHF band (0,03-0,30 GHz) and two fifth-order peaks in the S band (2.0 - 4.0 GHz) with the absorptivity over 90%.

+ The flexible, multi-band H-MPA with folded ring resonant structure: there are one fundamental peak in the UHF band (0,3 – 1,0 GHz) and one third-order peak in the L band (0.3 - 2.0 GHz) with the absorption of 99%. The absorption properties of the high-order absorption peak are well maintained in both cases: the material is in flat and bent configurations.

+ Flexible H-MPA operating in the C (4,0-8,0 GHz) and X bands (8,0-12,0 GHz) with even-order magnetic resonance: The second-order magnetic resonance is excited in the bending configuration.

3. Expanding the study of some H-MPA structure operating in the higher frequency region (THz) to clarify the dependence of the absorption spectrum on the curvature states. In flat state, the absorption reaches over 96% at 34.9 THz (fundamental magnetic resonance) and 97.2 THz (third-order magnetic resonance). In different curvature states (bending radius varied from 50 to 5  $\mu\text{m}$ ), this H-MPA maintains the fundamental peak well with absorption above 90%. Specially, there is a new second-order resonance peak at 54.5 THz with absorption of about 80% when bending radius reduces to be 5  $\mu\text{m}$ .

### **PERSPECTIVE**

1. Continue to improve the resonant structures to obtain a multi-band/broadband H-MPA that uses both even- and odd-order resonances, stable under bending effects.
2. Study the integration of other advanced flexible dielectric materials into the H-MPA structure.
3. Investigate potential applications of H-MPAs in practice such as: Frequency filters and sensors.

## **LIST OF THE PUBLICATIONS RELATED TO THE DISSERTATION**

- 1. Duong Thi Ha**, Vu Thi Hong Hanh, Bui Son Tung, Nguyen Thi Hien, Dinh Ngoc Dung, Bui Xuan Khuyen, Liang Yao Chen, YoungPak Lee and Vu Dinh Lam, “*Ultrathin hybrid absorber based on high-order metamaterial*”, Journal of Optics **23**, 095101 (2021).
- 2. Duong Thi Ha**, Bui Son Tung, Bui Xuan Khuyen, Thanh Son Pham, Nguyen Thanh Tung, Nguyen Hoang Tung, Nguyen Thi Hoa, Vu Dinh Lam, Haiyu Zheng, Liangyao Chen and YoungPak Lee, “*Dual-Band, Polarization-Insensitive, Ultrathin and Flexible Metamaterial Absorber Based on High-Order Magnetic Resonance*”, Photonics **8**, 574 (2021).
- 3. Duong Thi Ha**, Vankham Boudthaly, Soulima Khamsadeth, Vu Thi Hong Hanh, Bui Son Tung, Bui Xuan Khuyen, Vu Dinh Lam, “*Mechanically tunable dual-band metamaterial absorber at ultra-high frequency*”, Tạp chí nghiên cứu KH&CN quân sự **84**, 93-100 (2022)
- 4. Duong Thi Ha**, Bui Xuan Khuyen, Bui Son Tung, Pham Thanh Son, Vu Thi Hong Hanh, Trinh Thi Giang, Nguyen Thanh Tung and Vu Dinh Lam, “*Mechanically-tunable metamaterial for multi-band absorption*”, TNU Journal of Science and Technology **228**(14): 142 – 151 (2023).
- 5. Duong Thi Ha**, Soulima KHAMSADETH, Vu Thi Hong Hanh, Nguyen Van Ngoc, Bui Son Tung, Bui Xuan Khuyen, vu Dinh Lam, “*Optimization of narrow-band thermal emission based on flexible metamaterials*”, The National Conference on Solid State Physics and Materials Science 13 (SPMS 2023), 5-7/11, Ho Chi Minh, Vietnam, 2: 690-697 (2023). ISBN 978-604-471-703-6.